

See discussions, stats, and author profiles for this publication at: <https://www.researchgate.net/publication/23476598>

Energetics and Structures of Charged Helium Clusters: Comparing Stabilities of Dimer and Trimer Cationic Cores

ARTICLE *in* CHEMPHYSICHEM · DECEMBER 2008

Impact Factor: 3.42 · DOI: 10.1002/cphc.200800457 · Source: PubMed

CITATIONS

8

READS

13

4 AUTHORS, INCLUDING:



[Enrico Bodo](#)

Sapienza University of Rome

111 PUBLICATIONS 1,536 CITATIONS

SEE PROFILE



[Franco A Gianturco](#)

Sapienza University of Rome

448 PUBLICATIONS 6,214 CITATIONS

SEE PROFILE



[Ersin Yurtsever](#)

Koc University

138 PUBLICATIONS 1,229 CITATIONS

SEE PROFILE

Energetics and Structures of Charged Helium Clusters: Comparing Stabilities of Dimer and Trimer Cationic Cores

Fabio Marinetti,^[a] Enrico Bodo,^[a] Franco A. Gianturco,^{*,[a]} and Ersin Yurtsever^[b]

We present accurate ab initio calculations of the most stable structures of He_n^+ clusters in order to determine the more likely ionic core arrangements existing after reaching structural equilibrium of the clusters. Two potential energy surfaces are presented: one for the He_2^+ and the other with the He_3^+ linear ion, both interacting with one He atom. The two computed potentials are in turn employed within a classical structure optimization where the overall interaction forces are obtained within the sum-of-potentials approximation described in the main text. Because of

the presence of many-body effects within the ionic core, we find that the arrangements with He_3^+ as a core turn out to be energetically preferred, leading to the formation of $\text{He}_3^+(\text{He})_{n-3}$ stable aggregates. Nanoscopic considerations about the relative stability of clusters with the two different cores are shown to give us new information on the dynamical processes observed in the impact ionization experiments of pure helium clusters and the importance of pre-equilibrium evaporation of the ionic dimers in the ionized clusters.

1. Introduction

The ionized clusters of neat helium, especially those with a relatively small number n of atoms, are among the simplest of the increasing number of ionic clusters containing both atomic and molecular ions which have recently received attention both from experimental and theoretical studies.^[1,2] One of the goals of such studies has been to complement the vast wealth of information on neutral van der Waals (vdW) molecules accumulated over the last 20 years, with the assembly of comparable data on ionic clusters. In fact, the combined use of several spectroscopic methods, has enabled the provision of direct information on structures, binding energies, and inter- and intramolecular vibrations in clusters of varying size, thereby acquiring a more detailed understanding of the way in which charged and neutral species interact at close range.^[3,4]

The onset of the ionization process in ^4He clusters, either in neat clusters or in those doped by atoms and molecules, strongly modifies the network of the bonds associated with the aggregate components before that process, since the original vdW interactions are now replaced, at least around the new core, by forces of near-chemical strength which tend to increase the density of the adatoms around the charged region (electrostriction) and further enhance the formation of regular, solid-like configurations of the solvent (snowballs).^[5,6] One of the most intriguing questions about the structures of such clusters, especially for the pure ^4He aggregates which we discuss herein, is related to establishing the features of the ionic core within the cluster itself, since the initial charge is expected to eventually become localized over a relatively small number of more strongly bound atoms, while the residual solvent environment is attached to this core by induction and dispersion effects.^[7]

Earlier experimental studies^[8–11] on the non-equilibrium fragmentation of charged He clusters suggested a predominance of the He_2^+ signal after fragmentation, the coexistence of He_3^+

and He_2^+ signals for the smaller size ranges and the reduction of the signal from the He_3^+ cores in the larger clusters, while the He_2^+ signal remained strong and dominant. Such behavior was also surmised by earlier diatomic-in-molecule (DIM) calculations,^[12] although further studies on the computational side have questioned^[13] the reliability of the DIM approximation for treating noble gas ionic aggregates. The actual structures of the ionic, final equilibration of the charged “islands” (i.e. of the expected ionic cores) in such ionized clusters is therefore still under debate, because it is not entirely clear how the large energy excess after ionization can be dissipated within the cluster.^[14] However, it has become accepted that the aggregate probably evolves through some metastable path where a fairly small ionic core is formed^[10] and that the latter is likely to be excited into some vibrationally high internal state, initially populated via the excess energy deposited by the primary ionization which thermalizes within the solvent network by following several evaporative cooling channels. Such a qualitative picture may in turn be used to explain the large rates of evaporation of the He droplets after ionization^[10,11] and the fact that the dimer and trimer ionic fragments (with a predominance of the first in all size aggregates) give rise to strong peaks in the mass spectra.^[10,11] It is also interesting to note that earlier, similar studies for Ar ionic clusters^[15,16] have found

[a] F. Marinetti, Dr. E. Bodo, Prof. F. A. Gianturco
Department of Chemistry
University of Rome “La Sapienza” and CNISM
Piazzale A. Moro 5, 00185 Rome (Italy)
Fax: (+39) 06-49913305
E-mail: fa.gianturco@caspur.it

[b] Prof. E. Yurtsever
Chemistry Department
Koç University, Istanbul 34450 (Turkey)

the trimer ion to be the more stable core of its more strongly bound aggregates.

In earlier computational studies^[17–19] on He_n^+ , we have analyzed in detail the structural features of a vibrationally excited dimer core, $^4\text{He}_2^+$ ($v \gg 0$), interacting with a ^4He atom and discussed the collisional efficiency of its cooling within the droplet by energy transfer processes induced by multiple collisions. We have also studied the bound state structures of the full He_3^+ complex whose transient formation within the cluster had been surmised earlier.^[18] From ab initio calculations we have further analysed the effect of charge migration within the He_3^+ system upon distortion of its linear structures.^[19] The picture emerging from those studies is one in which the He_2^+ species has a strong possibility of stabilizing within the core region of the droplet after undergoing internal energy dissipation via multiple collisions, and hence by multiple evaporative cooling events, with the surrounding adatoms of the ^4He droplet.

Herein, we wish to extend the above findings further by pursuing two different aspects of the problem which, as far as we are aware, have not yet been considered fully by computational studies. We start by analyzing which are the quantum-chemically optimized structures of small ionic clusters (with $n < 8$) in order to see the equilibrium stability of either dimer or trimer cores in their final equilibrium configurations at 0 K. To that aim, we computed a new potential energy surface associated with the equilibrated (“cold”) structure of $^4\text{He}_3^+$ (a linear molecule) interacting with ^4He and we carried out a structural comparison within a broad range of ionic clusters (up to $n \sim 30$) which could have either the dimer or the trimer ion as their central cores. This last analysis should help us to better understand the alternative energy pathways provided during the cluster stabilization processes after the initial formation of those ionic cores that are experimentally considered to be the most likely to occur and to survive after final cluster break-ups: He_2^+ and He_3^+ .

The purpose of this work is *not* to describe the actual dynamics of the system’s evolution, nor do we intend to see how the system modifies itself from the initial ionization up to the final collection of its fragments at the mass spectrometer. In our scheme, the final cluster quasi-equilibrium is one requirement we make as a starting condition of the calculations. We carry out our comparison to verify the relative stabilities of two possible cores in the clusters vis à vis the experimental findings, keeping in mind that to direct fully ab initio calculations of even larger clusters’ structural energies is still outside the capabilities of the available codes and that the very numerous, and possible, pathways which can follow several initial (non-equilibrium) setups of the clusters are not amenable to direct computation.

2. Ab Initio Structures: A Brief Description

The experiments^[10] carried out on the title systems show that the most important fragments collected at the end of the cluster break-ups are represented by the He_2^+ and the He_3^+ fragments, while no information is provided about the cores which

must exist in the larger clusters that survive after the fragmentation. Several theoretical studies^[12,21,18,20] have tried to provide this missing information. The results that have been found most often show the formation of a trimeric core for the smaller clusters but, as one continues the series, the increase in the number of degrees of freedom and in structural complexity of the systems make the dimeric core become a more competitive arrangement in the clusters.^[12]

In order to get a firm reference from which we carry on our further analysis, we completed a series of new ab initio structural optimizations of the system He_n^+ where n varies between 3 and 7. We used the Gaussian 03 suite of codes,^[22] applying Møller–Plesset perturbation theory as implemented in the MP4(SDQ) method with the aug-cc-pVTZ basis set. The minimum energy structures resulting from the calculations are shown in Figure 1. Since the preliminary calculations were only

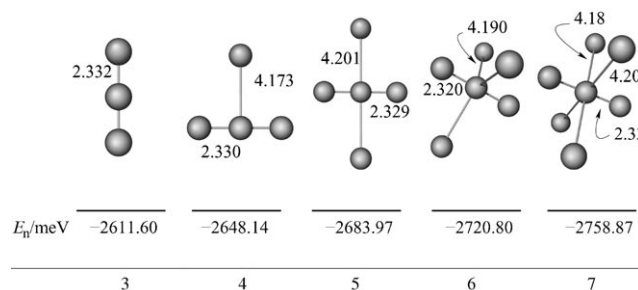


Figure 1. Optimized ab initio structures for He_n^+ clusters for $n=3-7$. Each distance is shown close to the relevant bond. Values are in a.u. The symmetry groups of the structures are, from left to right: $D_{\infty h}$, C_{2v} , D_{2h} , D_{3h} , D_{4h} .

intended to illustrate the relative behaviour of the smaller clusters (before embarking on the optimization study with full PESs) we did not deem it necessary to employ larger basis sets for the MP4 calculations in order to assess the energy convergence level. However, we are aware of the presence of size-consistency errors, which we estimate to be about 20 meV in this case.

As shown in the figure, all the most stable clusters present a trimeric core, the shape of which essentially remains unaffected upon addition of extra helium atoms. This finding also agrees with the results already obtained in ref. [12]. This indicates that the “chemical affinity” for other He atoms, which should cause an extension of the charge migration and the charge sharing effects in larger clusters, is completed after three atoms and therefore, from that size on, the system behaves as a VdW complex where the induction and dispersion forces between the ionic core and the remaining neutral He atoms dominate the attachment energies of the additional cluster atoms.

3. The Sum-of-Potential Approximation and its Limits

The previous results gave us only preliminary indications about the features of the ionic systems and need to be further re-

finied. The procedure we used for the present He_n^+ cluster studies has been widely employed by us for various He-containing systems. It consists of first calculating the whole potential energy surface (PES) for the ensemble “core+He” and, once fitted with a suitable analytical formula, we then use it to evaluate the total cluster binding energy as a sum of two-body terms as in Equation (1):

$$V = \sum_{i=N} \left[V_{\text{core-He}}(\mathbf{R}_i) + \sum_{i<j}^N V_{\text{He-He}}(r_{ij}) \right] \quad (1)$$

We have followed the above steps for the two different kinds of ionic cores within the ^4He clusters by keeping their intramolecular distances at their isolated equilibrium values. The above approximation turns out to be very effective when weakly interacting dopants are present in a cluster which is a neutral solvent^[23] and it has also been extended to clusters containing an ionic core.^[5,24,25] In the latter instance, however, the absolute energy values are slightly smaller than those from full ab initio data, although the overall structural patterns remain the same.^[24,25] Based on this, we consider the usage of the sum-of-potential scheme to be a realistic structural tool for analyzing large clusters with mixed vdW and ionic interactions.

3.1. He_2^+He

The He_2^+He PES has been already evaluated by Scifoni et al.,^[18] so that we refer to that work for the computational details. Herein we only show a mapping of energy isolines in Figure 2.

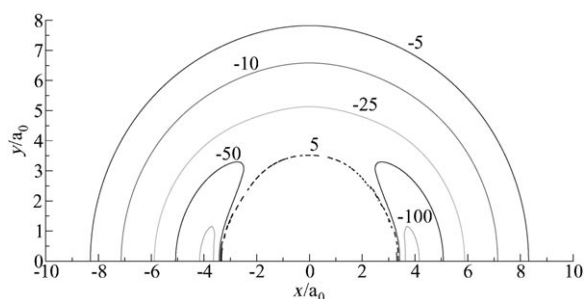


Figure 2. Two-dimensional energy isolines for the He_2^+He PES. Energy values are in meV. The ionic dimer mid-bond position is placed at $x=0$.

The absolute minimum of the PES is a collinear arrangement at a distance of $3.8 a_0$ with an energy value of -117.43 meV. The shape of the surface presents a clear orientational anisotropy as the Jacobi angle moves from 0° to 90° , as shown in Figure 3. This is due to charge-migration effects, which are preferential in the collinear orientation of the complex. The corresponding zero point energy (ZPE) of the system is about 43.8 meV.^[18] By analyzing the Mulliken charge distribution (not shown here) we can see that when the third He atom approaches the dimeric core from the collinear direction, the system takes up a symmetric geometry that describes two equivalent He_2^+ subaggregates. For this reason, part of the

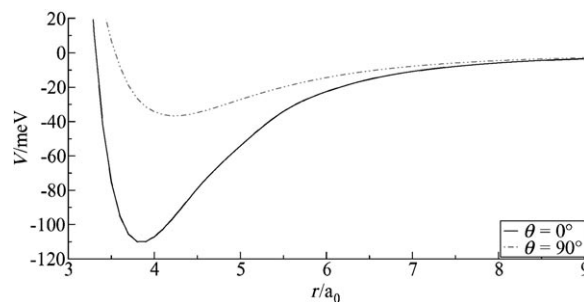


Figure 3. Linear cuts of the He_2^+He PES. Distances are in a.u. and energies in meV. The distances are measured from the midpoint of the He_2^+ bond length.

original positive charge migrates onto the third atom. However, when the He adatom approaches along the $\theta=90^\circ$ insertion path, the charge is not shared with the incoming atom.^[17] The He_2^+ intramolecular distance has been frozen at its equilibrium value ($2.04 a_0$), although it is worth mentioning that the stretching of this coordinate dramatically changes the magnitude of the interaction due to the formation of an He_3^+ -like complex which is stabilized by charge sharing between the two wing atoms and the central one. This effect is specific for a single adatom interacting with the He_2^+ and is not additive. Thus, the inclusion of this contribution in Equation (1) causes a large overestimation of the total interaction energy.

3.2. He_3^+He

The He_3^+He PES was evaluated by carrying out single-point calculations for a broad range of positions of the fourth He atom. The He_3^+ geometry has been taken to be fixed at its equilibrium structure which is linear and symmetric, with the He–He distances equal to $2.34 a_0$.

The calculations were carried out at the MP4 level with the aug-cc-pVQZ basis set using the Gaussian 03 suite of codes.^[22] All the results have then been fitted with an analytical formula by using the same procedure adopted in our earlier work (see for example refs. [24,25]). The long-range part of our potential has the behaviour expected from the induction and dispersion contributions which appear in Equation (2):

$$V_{\text{LR}} = -\frac{af_4(\beta R)}{2R^4} + \frac{f_6(\beta R)}{R^6} [C_{60} + C_{62}P_2(\cos \theta)] \quad (2)$$

where the Tang–Toennies coefficient $f_N(\beta R)$ ^[26] correctly quenches the long-range potential in the short-range region.

Figure 4 shows that the minimum energy position of this PES is at 90° with respect to the molecular axis, indicating a marked difference from the He_2^+ core. Furthermore, the interaction energy is, in general, smaller than in the former case since the complex of He_3^+ with a neutral He is more likely to resemble a vdW complex: its core has lost the capability of forming an additional “chemical” bond via charge-sharing processes because of the “charge saturation” effect.

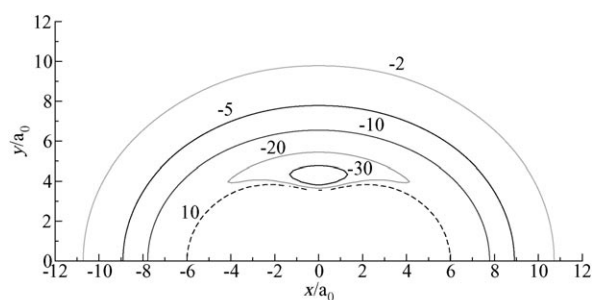


Figure 4. Two-dimensional energy isoline representation of the He_3^+He PES. Distances are in a.u. and energy values are in meV. The $x=0$ position is that of the central atom of the trimer ion.

The position of the PES minimum also reflects the Mulliken charge analysis for He_3^+ in its equilibrium geometry (not reported here), which shows the largest part of the positive charge residing on the central atom.^[17] Therefore, the charge distribution indicates the central atom of the trimer as the strongest interacting center in the core, with the $\theta=90^\circ$ configuration becoming the lowest energy arrangement of the PES. The collinear geometry therefore places the fourth He atom far from the center of the trimer and the corresponding interaction energy is more repulsive, leading to weaker interaction forces.

Thus, the most stable arrangement of the He_3^+He cluster is the T orientation, with the fourth He atom at a distance of about $4.2 a_0$, where the energy value is -36.2 meV. This difference in energy, with respect to the value we found for the He_2^+He system, indicates a saturation of the “reactive system” (the core), which reaches its stablest charge distribution in the He_3^+ trimer. It therefore does not undergo any additional charge transfer to neighbouring He atoms as the droplet grows in size. It is also worth mentioning that the ZPE value for this system is now about 12 meV, that is, much smaller than in the case of the dimer core potential. This means that both systems exhibit similar percentage values for the ZPE while the dimer core structures have much larger stabilization energies. This feature plays a role in the relative comparisons of the larger clusters.

3.3. The Breakdown of the Sum of Potential Approximation

After the calculation of the PES described above, the ensuing step was to obtain the total energies for the many possible configurations of the clusters with both cores (dimer or trimer ions) in order to extract the total binding energies for the most stable clusters. We carried out this task by expressing the overall potential as a sum of two-body terms as indicated in Equation (1) and neglecting the many-body (MB) effects in the make-up of the full interaction.

Our previous experience with neutral and ionic systems^[24,25,27,28] has already suggested to us that the neglected terms are not large and therefore that both the structures and the total energies, when corrected for the MB effects, are close to their approximate values given by Equation (1). This is par-

ticularly true for the vdW complexes where the interaction forces are not strong and the many-body effects are chiefly related to the dispersion and induction forces that essentially vanish as the distances become large.

In the present case we have two different situations: the formation of a dimeric core which has a sort of “chemical affinity” for other He atoms, and the case of the “charge-saturated” trimer ionic core, which behaves with the adatoms as in vdW complexes. Thus, we need to check the validity of the sum-of-potentials approximation in order to make the correct comparison between the energies of the two series of ionic clusters with different cores. The way we have chosen to achieve this comparison is described by the following steps:

1. The optimized structures of both cluster series are compared with single-point ab initio calculations at the same geometries, so that MB effects are included;
2. The difference between the SOP energies and the ab initio energies is therefore defined as the missing MB contributions according to Equation (3) for a cluster of size n :

$$E_{\text{MB}}^n = E_{\text{abinitio}}^n - E_{\text{SOP}}^n \quad (3)$$

3. The cluster total binding energy is then shifted by taking into account the MB effects of Equation (3) for each considered size. The calculation was done at the MP4/aug-cc-pVQZ level of theory.

In Table 1 we report the values of the MB energy for some selected clusters sizes. In the case of $\text{He}_3^+(\text{He})_{n-3}$ these effects induce a relatively small and constant correction. This indicates that the clusters behave similar to vdW aggregates. On the

Table 1. Many-body energy contributions calculated as described in Equation (3) for the $\text{He}_2^+(\text{He})_{n-2}$ and $\text{He}_3^+(\text{He})_{n-3}$ clusters of different sizes. E_{MB}^n are given in meV.

n	$\text{He}_2^+(\text{He})_{n-2}$	$\text{He}_3^+(\text{He})_{n-3}$
4	97.32	5.14
5	98.30	5.33
6	99.76	5.07
7	101.68	4.71

other hand, the $\text{He}_2^+(\text{He})_{n-2}$ have a large energy contribution coming from MB effects, a result that indicates that the systems with the dimer ion core are not described well by a SOP potential such as that of Equation (1). However, the correction remains almost constant along the series of small clusters considered herein, and it is mainly due to the formation of the linear complex $\text{He}_2^+(\text{He})_2$ which is a typical core substructure formed in the smaller clusters under consideration, as shown in Figure 5. The linear subcomplex $\text{He}_2^+(\text{He})_2$ also occur for the larger clusters, as shown in Figure 6 for two of the cases examined herein. In other words, the two distinct series of clusters with different ionic cores show very different MB energy-cor-

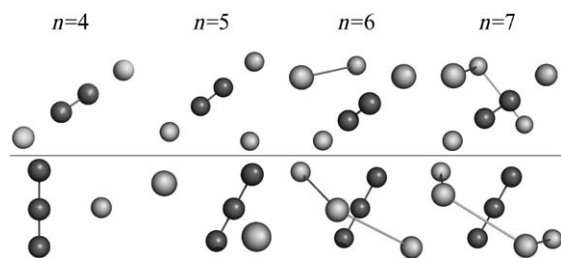


Figure 5. Geometries of the He_n^+ clusters ($n=4-7$). The upper panel shows the series with the dimeric core, while the lower panel shows the series with the trimeric core.

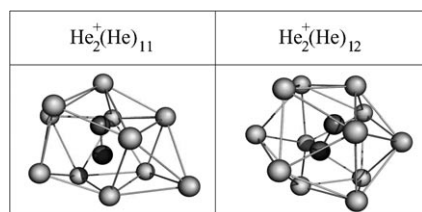


Figure 6. Clusters $\text{He}_2^+(\text{He})_{11}$ and $\text{He}_2^+(\text{He})_{12}$. Both of them show the formation of the linear subcomplex $\text{He}_2^+(\text{He})_2$.

reaction effects, while also indicating that such effects are confined to the inner ionic cores. Thus, these energy-corrections are largely size-independent within each series of ionized clusters. We can interpret the difference in energy behavior by noting that the first adatom (the one which first forms He_2^+ He) can be considered to form a chemical bond with the ionic core because of the open-shell nature of the latter and of the charge-sharing effect that this feature causes. When we add a fourth atom, within the potential model of Equation (1), this sets itself in an equivalent position as the third one and with the same energy gain. However, this result does not correspond to the true energy situation in that geometry, since the SOP energy should be less negative because only one of the two He adatoms benefits from the quasi-chemical interaction with the He_2^+ core. Thus, the greatest part of the missing MB energy in the clusters with the He_2^+ core is due to the error made when considering the He_2^+He PES as the building-block contribution in Equation (1). The latter PES, in fact, incorrectly considers the third and the fourth atoms as being energetically equivalent in their contributions to cluster stability.

4. A Comparison of Competitive Energetic Behavior

Once able to assemble the overall potential energy surfaces for the two systems (He_2^+He_n and He_3^+He_n), we can use the final potential functions for structure and energy optimizations. Details about our optimization procedure and code have been discussed extensively in an earlier work.^[27] Shortly, we use a genetic algorithm approach based on our proprietary code (GeCO) which is able to find the lowest energy minimum of a system with a large number of degrees of freedom. The

output of the program provides both the lowest (classical) energy and the spatial arrangements of the clusters. Both these features are compared and analyzed in the following.

Figure 7 shows the energy profile for the growth of the two different cluster series. The two horizontal black lines identify the energy of the ionic diatom He_2^+ at two different values of

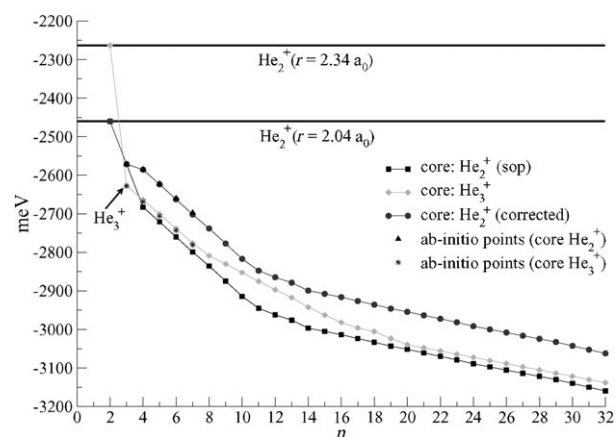


Figure 7. Calculated total energies of the He_n^+ systems with n up to 32. The asymptotic energies refer to the completely dissociated system $\text{He}^+ + n\text{He}$.

internuclear distance: $2.04 a_0$, which is the equilibrium value, and $2.34 a_0$, which is the He–He distance in He_3^+ . Thus, the He_2^+ series dissociates at the former geometry while the He_3^+ series dissociates at the latter one. In the same figure, we have reported the following different situations: the sum-of-potentials for He_3^+ , the corrected sum-of-potentials for the He_2^+ core, and the ab initio calculations. They are plotted in order to underscore the very good agreement between the different approaches which we found in the present study. Furthermore an uncorrected sum-of-potentials profile for the dimeric core is drawn in order to show the error in the energy we would have if we did not include the MB term of Equation (3).

The comparison between the energies of the two series of clusters shows the following situation: the “chemical” affinity of He_2^+ is not totally screened by other He adatoms, and consequently the dimeric core artificially shows a higher stability when binding to more than one of the surrounding He adatoms, thereby “falsely” trying to create several He_3^+ subsystems. As a consequence, and as shown by the calculations of Figure 7, the more stable clusters seem to be those with the dimer core unless the MB effects are correctly included: this means that all SOP values are shifted upwards by 93.7 meV. Once we have done that, the He_2^+ -core series (■ in Figure 7) is higher in energy (●) than the He_3^+ -core progression (◆). Therefore, our final calculations clearly show now that the trimer-core-containing clusters become those which are more strongly bound along the series. Hence, once the system reaches its equilibrium, we find that the surviving clusters should have He_3^+ as a solvated ionic core. Also, the larger basis sets employed in the calculations of Table 1 are now producing total energies lower than those reported in Figure 1.

The small changes, however, do not modify the physical picture outlined herein.

Another interesting quantity which provides us with further stability indications in a cluster series is the single-atom evaporation energy (E_{evap}^n) obtained as a difference in total energies $E_n - E_{n-1}$, shown in Figure 8. The two cluster series now have

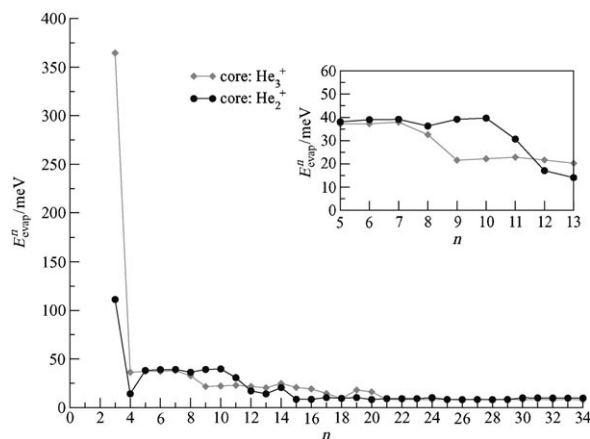


Figure 8. Calculated single-atom evaporation energy as a function of the cluster size. Inset: Stabilization energy of the symmetric He_3^+ complex with respect to He_2^+He .

very similar E_{evap}^n values for all the values of n but the first one ($n=3$). This reflects the larger stabilization energy of the symmetric He_3^+ complex with respect to He_2^+He , as given by the top value in the Figure and for the reasons we discussed before. From the evaporation energy behavior, therefore, there is no clear preference for one core with respect to the other, because the detachment of one He atom from a cluster requires approximately the same amount of energy for both types of ionic cores. Thus, we conclude that the evolution of the equilibrated systems should be largely the same for clusters with either core, because the evaporation of the He adatoms requires the same energy within our present modeling of its energetics.

Under the working conditions of the experiments described in ref. [10], one starts with an initially neutral cluster He_n of size n that is ionized. It then forms $(\text{He}_n^+)^*$ and undergoes fragmentation due to the energy release from the cooling of the newly formed core molecular ion. The final fragments that still bear a positive charge are then collected at the mass spectrometer. The results we have obtained from our equilibrium calculations therefore suggest that the stablest aggregates from the initial He_n^+ cluster should equilibrate with a trimeric core. On the other hand, we should also expect that the probability of finding a fragment with $n \geq 3$ should increase as n increases, because the available energy release may not be sufficient to fully evaporate all the He adatoms attached to the core. The consequence of this is that, if the experiments were to monitor near-equilibrium situations they should also find He_n^+ fragments with $n \geq 3$ that become larger as n increases. This is not, however, what is experimentally observed: ref. [10] suggested that the ionic dimer could be more easily ejected

during evaporation, thereby producing more He_2^+ fragments than we would expect to find from a purely incremental evaporative cooling process. Hence, the mechanism suggested by ref. [10], once combined with our present findings on the cluster energy, allows us to surmise that, given the greater stability of He_3^+ -containing clusters, the non-equilibrium process of prior, direct He_2^+ evaporation from the cluster (as also suggested in ref. [10]) can occur together with the stripping mechanism of an equilibrated species, thereby enhancing the efficiency of ejecting He_2^+ as the cluster size increases and causing detection of the dominant ionic dimer fragmentations as seen in ref. [10].

5. Conclusions

When analysing the fragmentation of ionized He clusters, earlier studies^[18,29,10] have proposed a series of possible nanoscopic mechanisms that can occur during the entire dynamic process, from the initial ionization to the final equilibrium structures of the cluster. The experimental data suggest two possible paths. The first possibility is that the charge migrates towards the center of the cluster via resonant charge-transfer and there forms a vibrationally excited He_2^+ core which is in turn stabilized by an evaporative cooling mechanism. Another suggested path is one where the “hot” He_2^+ is formed on the surface of the cluster and is then ejected from it during the relaxation process and before completing the overall equilibration of the residual structure.

Herein, we analysed the ionization of the small clusters by looking at the final, equilibrated cluster structural energy obtained after its optimization in the presence of two competing cores. The systems were also studied first by using ab initio calculations in order to understand the features of the overall interactions and the importance of the many-body effects. Different ab initio PESs were additionally generated by selecting two of the possible ionic cores which the experiments indicated as being the most probable to be left after cluster fragmentation. In other words, we focused our calculations on the species suggested by the experiments to be the most abundant. The correctness of using them within the sum-of-potential approximation was also discussed and full geometry optimizations of the He_n^+ clusters containing both possible ionic cores were carried out and a comparison between their relative energetics was made for their equilibrium configurations at 0 K.

The results show that the cluster series with a trimer core has the larger stabilization energy and therefore should be enthalpically favoured, thereby causing the more abundant fragments to be either the He_3^+ residues or those with the He_3^+ as their core. Within this hypothesis, one would also expect that the mass spectrometer signals coming from these species should increase with respect to the He_2^+ as the observed cluster size increases. The experiments reveal instead that the size of the He_3^+ signal is approximately a constant as n increases while the one due to the He_2^+ fragments increases with n .

This suggests that the observed, sizeable amount of He_2^+ fragments could not be produced only by sequential evaporative cooling of stabilized structures, because this path would

reach equilibrium structures with energy differences similar to those calculated herein and therefore would provide an increasing signal for He_3^+ fragments as the cluster size increases. It therefore follows that the signal from an initially formed He_2^+ core would be observed to increase in size when n increases if, during the non-equilibrium period, dynamic evolution were to reach the cluster surface and undergo ejection before being able to stabilize into the energetically favoured He_3^+ core found by our calculations. In other words, the preferential stabilization of the latter core (once equilibrium is reached) indicates that another competing mechanism of dimer core evaporation during non-equilibrium evolution of the ionic droplets has to be active in order to offset the energy-favoured trimer core formation upon equilibration of the ionized clusters.

We think, in conclusion, that the present study of the equilibrium energetics of the two possible, and most probable, cores in ionized He clusters allows us to find further support for the presence of important pre-equilibrium evaporative losses from the initially formed clusters, in accord with experimental suggestions,^[10] and also allows us to suggest that upon equilibration of the ionized clusters the trimer ionic core should be the more abundant residual species. The latter finding would be validated by a different type of experimental searches, for example, those where chiefly equilibrated clusters are analyzed by delayed observation.

Acknowledgements

The financial support from the Research Committee of the University of Rome, and from the PRIN 2006 projects from the Ministry of University and Research are all gratefully acknowledged. The computational support from the CASPUR supercomputing consortium is also acknowledged here.

Keywords: ab initio calculations • cations • cluster compounds • helium • van der Waals complexes

- [1] for example, see: *Clusters of Atoms and Molecules, Vol. I and II* (Ed.: H. Haberland), Springer, Berlin, **1994**.
- [2] E. J. Bieske, O. Dopfer, *Chem. Rev.* **2000**, *100*, 3963–3998.
- [3] *Cluster Ions* (Eds.: C.-Y. Ng, T. Baer, I. Powis), Wiley, New York, **1993**.
- [4] J. P. Maier, *Ions and Cluster Ions Spectroscopy and Structure*, Elsevier, Amsterdam, **1989**.
- [5] for example, see: B. Balta, F. A. Gianturco, F. Paesani, *Chem. Phys.* **2000**, *254*, 215–229.
- [6] F. Stienkemeier, A. Vilesov, *J. Chem. Phys.* **2001**, *115*, 10119–10137.
- [7] J. H. Kim, D. S. Peterka, C. C. Wang, D. M. Neumark, *J. Chem. Phys.* **2006**, *124*, 214301–214309.
- [8] H. Buchenau, E. L. Knuth, J. A. Northby, J. P. Toennies, C. Winkler, *J. Chem. Phys.* **1990**, *92*, 6875–6889.
- [9] H. Buchenau, J. A. Northby, J. P. Toennies, *J. Chem. Phys.* **1991**, *95*, 8134–8148.
- [10] B. E. Callicoatt, K. Foerde, L. F. Jung, T. Ruchti, K. C. Janda, *J. Chem. Phys.* **1998**, *109*, 10195–10200.
- [11] M. Ovchinnikov, B. L. Grigorenko, K. C. Janda, V. A. Apkarian, *J. Chem. Phys.* **1998**, *108*, 9351–9361.
- [12] P. J. Knowles, J. N. Murrell, *Mol. Phys.* **1996**, *87*, 827–833.
- [13] F. X. Gadea, I. Paidarova, *Chem. Phys.* **1996**, *209*, 281–290.
- [14] H. Haberland, B. V. Issendorff, R. Froehnticht, J. P. Toennies, *J. Chem. Phys.* **1995**, *102*, 8773–8779.
- [15] F. A. Gianturco, E. Buonomo, G. Delgado-Barrio, S. Miret-Artes, P. Villarreal, *Z. Phys. D* **1995**, *35*, 115–124.
- [16] F. Calvo, F. X. Gadea, A. Lombardi, V. Aquilanti, *J. Chem. Phys.* **2006**, *125*, 114307–114319.
- [17] E. Scifoni, F. A. Gianturco, *Eur. Phys. J. D* **2002**, *21*, 323–333.
- [18] E. Scifoni, G. Dellepiane, F. A. Gianturco, *Eur. Phys. J. D* **2004**, *30*, 353–362.
- [19] E. Scifoni, E. Bodo, G. Dellepiane, F. A. Gianturco, *Eur. Phys. J. D* **2004**, *30*, 363–368.
- [20] M. Rosi, C. W. Bauschlicher, Jr., *Chem. Phys. Lett.* **1989**, *159*, 479–484.
- [21] F. A. Gianturco, M. P. De Lara-Castells, *Int. J. Quantum Chem.* **1996**, *60*, 593–608.
- [22] M. J. Frisch, G. W. Trucks, H. B. Schlegel, G. E. Scuseria, M. A. Robb, J. R. Cheeseman, J. A. Montgomery, Jr., T. Vreven, K. N. Kudin, J. C. Burant, J. M. Millam, S. S. Iyengar, J. Tomasi, V. Barone, B. Mennucci, M. Cossi, G. Scalmani, N. Rega, G. A. Petersson, H. Nakatsuji, M. Hada, M. Ehara, K. Toyota, R. Fukuda, J. Hasegawa, M. Ishida, T. Nakajima, Y. Honda, O. Kitao, H. Nakai, M. Klene, X. Li, J. E. Knox, H. P. Hratchian, J. B. Cross, V. Bakken, C. Adamo, J. Jaramillo, R. Gomperts, R. E. Stratmann, O. Yazyev, A. J. Austin, R. Cammi, C. Pomelli, J. W. Ochterski, P. Y. Ayala, K. Morokuma, G. A. Voth, P. Salvador, J. J. Dannenberg, V. G. Zakrzewski, S. Dapprich, A. D. Daniels, M. C. Strain, O. Farkas, D. K. Malick, A. D. Rabuck, K. Raghavachari, J. B. Foresman, J. V. Ortiz, Q. Cui, A. G. Baboul, S. Clifford, J. Cioslowski, B. B. Stefanov, G. Liu, A. Liashenko, P. Piskorz, I. Komaromi, R. L. Martin, D. J. Fox, T. Keith, M. A. Al-Laham, C. Y. Peng, A. Nanayakkara, M. Challacombe, P. M. W. Gill, B. Johnson, W. Chen, M. W. Wong, C. Gonzalez, J. A. Pople, *Gaussian 03 (Revision C.02)*, Gaussian, Inc., Wallingford, CT, **2004**.
- [23] F. Paesani, F. A. Gianturco, *J. Chem. Phys.* **2002**, *116*, 10170–10182.
- [24] E. Bodo, F. A. Gianturco, E. Yurtsever, M. Yurtsever, *Mol. Phys.* **2005**, *103*, 3223–3231.
- [25] E. Bodo, E. Yurtsever, M. Yurtsever, F. A. Gianturco, *J. Chem. Phys.* **2006**, *124*, 074320–074332.
- [26] U. Kleinekathöfer, K. T. Tang, J. P. Toennies, C. L. Yiu, *Chem. Phys. Lett.* **1996**, *249*, 257–263.
- [27] For example, see our earlier application in: F. Marinetti, E. Bodo, F. A. Gianturco, *ChemPhysChem* **2007**, *8*, 93–100.
- [28] F. Marinetti, E. Bodo, F. A. Gianturco, *J. Theor. Comput. Chem.* **2006**, *5*, 543–564.
- [29] J. Seong, K. C. Janda, N. Halberstadt, F. Spiegelmann, *J. Chem. Phys.* **1998**, *109*, 10873–10884.

Received: July 22, 2008

Revised: September 24, 2008